ANALYSIS OF COMBUSTION PERFORMANCE AND EMISSION OF EXTENDED EXPANSION CYCLE AND iEGR FOR LOW HEAT REJECTION TURBOCHARGED DIRECT INJECTION DIESEL ENGINES

by

Mohd F. SHABIR [a], Baluchamy Rajendra PRASATH [b*], and Packirisamy TAMILPORAI [c]

[a] Department of Mechanical Engineering, Aalim Muhammad Salegh College of Engineering, Chennai, India
[b] Department of Mechanical Engineering, Fatima Michael College of Engineering and Technology, Madura, India
[c] Department of Mechanical Engineering, Anna University, Chennai, India

Original scientific paper
DOI: 10.2298/TSCI130707012S

Increasing thermal efficiency in diesel engines through low heat rejection concept is a feasible technique. In low heat rejection engines the high heat evolution is achieved by insulating the combustion chamber surfaces and coolant side of the cylinder with partially stabilized zirconia of 0.5 mm thickness and the effective utilization of this heat depend on the engine design and operating conditions. To make the low heat rejection engines more suitable for automobile and stationary applications, the extended expansion was introduced by modifying the inlet cam for late closing of intake valve through Miller's cycle for extended expansion. Through the extended expansion concept the actual work done increases, exhaust blow-down loss reduced and the thermal efficiency of the low heat rejection engine is improved. In low heat rejection engines, the formation of nitric oxide is more, to reduce the nitric oxide emission, the internal exhaust gas re-circulation is incorporated using modified exhaust cam with secondary lobe. Modifications of gas exchange with internal exhaust gas re-circulation resulted in decrease in nitric oxide emissions. In this work, the parametric studies were carried out both theoretically and experimentally. The combustion, performance and emission parameters were studied and were found to be satisfactory.

Key words: *low heat rejection, Miller cycle, exhaust gas re-circulation, oxides of nitrogen*

Introduction

Low heat rejection (LHR) is one of the energy conservation concepts used in turbocharged diesel engines which results in low fuel consumption for the same power output, thereby reducing its size and aids to eliminate the cooling system. The diesel engine with its combustion chamber walls are insulated by heat flow resistant coating is referred to as LHR engine. The heat resistant coating reduces the heat transfer to the coolant system and improves the thermal efficiency by increasing the energy availability in the exhaust [1-7]. Turbocharging can prevent the deterioration in volumetric efficiency of the LHR engine and that there can be more effective utilization of the exhaust gas energy [8-10].

The engine with higher expansion ratio than compression ratio is referred to as extended expanded engine (EEE) [11]. The fundamental aim of extended expansion concept is to

* Corresponding author: e-mail: br_prasath@rediffmail.com

achieve higher work done by decreasing the compression work done, which in turn leads to higher thermal efficiency. This concept is compatible with the application of turbocharger and LHR engine. The short compression stroke is achieved by closing the intake valve early in the cycle before bottom dead centre (BDC) or by closing it late after BDC. The advantages of an extended expansion cycle includes, reduced specific fuel consumption and increased power output without increasing the cylinder peak pressure [12, 13]. LHR engine with exhaust gas re-circulation (EGR) gives good agreement in view of performance and emission characteristics [14, 15]. Also, the extended expansion cycle has the potential for NO_x emission control due to lower cylinder gas temperature but better results can be obtained by reducing intake oxygen concentration with EGR [16-18]. Internal EGR (iEGR) can be achieved by delaying the opening of exhaust valve, early closing of the exhaust valve and secondary opening of the exhaust valve during the intake stroke [19, 20].

In the present work, the combined potential of extended expansion cycle and iEGR in LHR turbocharged engine has been assessed. As a part of the investigation, initially a simulation program was run to optimize the inlet valve closing timing and percentage of iEGR for LHR turbocharged engine for better performance and lower NO_x emission levels. Finally, experimental investigations were performed to validate the predicted values of combustion, heat transfer process, performance and emission characteristics.

Computer simulation using combustion, gas heat transfer and wall heat transfer models

The combustion model is based on the Whitehouse and Way model [21] through which the preparation rate and reaction rate were estimated and subsequently the heat release was calculated [22]. Annand's combined heat transfer model [23, 24] was used to estimate the total heat transfer. The Wall heat transfer model is based on the thermal network analogy proposed by Amann [25] and Miyairi [26]. The nitric oxide concentration was obtained using modified Zeldovich mechanism through equilibrium reaction kinetics [27]. Using the first law of thermodynamics along with various energy and enthalpy coefficients the cylinder pressure, heat release and temperatures are calculated [28].

In this simulation during the start of compression, the mole of different species that are considered to be present includes oxygen, nitrogen from intake and carbon dioxide. Water (gaseous), nitrogen and oxygen from the residual gases.

Heat transfer

The gas-wall heat transfer is found out using Annand's convective heat transfer model. A wall heat transfer model is used to find out the instantaneous wall temperature. First term of this equation shows that Prandtl number for the gases forming the cylinder contents will be approximately constant at a value 0.7, claims that Reynolds number is the major parameter affecting convection. The second is a straightforward radiation term assuming gray body radiation:

$$\frac{\mathrm{d}Q}{\mathrm{d}t} = ak\frac{\mathrm{Re}^{b}}{d}(T_{\mathrm{C}} - T_{\mathrm{W}}) + c(T_{\mathrm{C}}^{4} - T_{\mathrm{W}}^{4}) \tag{1}$$

Wall heat transfer model

This model is used to find out conductive heat transfer through cylinder to the coolant and thereby to find instantaneous wall temperature. Initial temperature is found out using the following expression:

$$T_{\mathrm{wi}} = T_{\mathrm{g}} - \left(\frac{Q_{\mathrm{w}}}{h_{\mathrm{g}} 2\pi r_1 l} \right) W \tag{2}$$

and

$$Q_{\mathrm{w}} = \left(\frac{T_{\mathrm{g}} - T_{\mathrm{w}}}{R} \right) \tag{3}$$

The total conductive resistance offered by the cylinder liner, piston rings, cylinder head, ceramic coating and piston for the heat transfer from cylinder gases to coolant is calculated using the expression:

$$R = \left(\frac{1}{h_{\mathrm{g}} 2\pi r_1 l} \right) + \left(\frac{1}{h_{\mathrm{c}} 2\pi r_3 l} \right) + \log_{\mathrm{e}} \left(\frac{\frac{r_2}{r_1}}{k_1 2\pi l_1} \right) + \log_{\mathrm{e}} \left(\frac{\frac{r_3}{r_4}}{k_{\mathrm{c}} 2\pi l_{\mathrm{c}}} \right) +$$
$$+ 3 \log_{\mathrm{e}} \left(\frac{\frac{r_5}{r_9}}{k_{\mathrm{r}} 2\pi l_{\mathrm{r}}} \right) + \log_{\mathrm{e}} \left(\frac{\frac{r_7}{r_8}}{k_{\mathrm{s}} 2\pi l_s} \right) + \left(\frac{r_7}{k_{\mathrm{p}} 2\pi r_7 T_{\mathrm{p}}} \right) \tag{4}$$

Mass of fuel injected

Considering that nozzle open area is constant during the injection period, mass of the fuel injected for each crank angle is calculated using the following expression:

$$m_{\mathrm{f}} = C_{\mathrm{D}} A_{\mathrm{n}} \sqrt{2\rho_{\mathrm{f}} \Delta P} \left(\frac{\Delta\theta}{360N} \right) \tag{5}$$

Preparation rate

The preparation rate depends on the mass of fuel injected in the cylinder upto the time of calculation and part of the fuel still available for preparation with respect to partial pressure of oxygen. The preparation rate was calculated using the following equation [21]:

$$P_{\mathrm{r}} = K M_i^{(1-x)} M_{\mathrm{u}}^{\mathrm{x}} P_{\mathrm{O_2}}^{\mathrm{L}} \tag{6}$$

$$K = 0.085 N^{0.414} M^{1.414} P_{\mathrm{i}}^{-1.414} h^{-1.414} d_{\mathrm{n}}^{-3.644} \tag{7}$$

Reaction rate

The reaction rate depends on the delay period, velocity of gas molecules, oxygen density and mass of unburnt fuel. The effect of delay period was evaluated by introducing a chemical reaction rate using an Arrhenius type expression. Assuming that the velocity of the gas molecule is proportional to the square root of the temperature, the density of oxygen is proportional to the partial pressure divided by the temperature, the unburnt fuel is given by $\int (P_{\mathrm{r}(\theta+1)} - R_{\mathrm{r}(\theta)}) \mathrm{d}\theta$. The reaction rate was calculated using the following expression [21]:

$$R_{\mathrm{r}(\theta+1)} = \frac{K' P_{\mathrm{O_2}}}{N\sqrt{T}} \mathrm{e}^{\frac{-act}{T}} \int (P_{\mathrm{r}(\theta+1)} - R_{\mathrm{r}(\theta)}) \mathrm{d}\theta \tag{8}$$

where K' is the reaction rate constant ($87 \cdot 10^{10}$ K$^{1/2}$/bar·s) and act – the activation energy for the total species ($1.65 \cdot 10^4$ K).

Nitric oxide formation

Initial nitric oxide formation rate is given by:

$$\frac{\mathrm{d}[\mathrm{NO}]}{\mathrm{d}t} = \frac{6\cdot 10^{16}}{\sqrt{T}} \exp\left(\frac{-69090}{T}\right) \sqrt{[\mathrm{O}_2]_e}\,[\mathrm{N}_2]_e \tag{9}$$

$$\frac{\mathrm{d}[\mathrm{NO}]}{\mathrm{d}t} = \frac{2R_1\left\{1-\dfrac{[\mathrm{NO}]}{[\mathrm{NO}]_\mathrm{e}}\right\}^2}{1+\dfrac{[\mathrm{NO}]_\mathrm{e}}{[\mathrm{NO}]}\dfrac{R_1}{R_2+R_3}} \tag{10}$$

Nitric oxide equilibrium concentrations are calculated by:

$$[\mathrm{NO}]_\mathrm{e} = 20.3 \exp\frac{-21650}{T} \sqrt{[\mathrm{O}_2]_\mathrm{e}[\mathrm{N}_2]_\mathrm{e}} \tag{11}$$

Gas exchange process

When the cylinder is open to the inlet system or the exhaust system or to both the systems, the cylinder conditions are affected by the flow conditions in the inlet and exhaust systems. Furthermore, the composition of the cylinder contents will vary with time. The gas exchange process commences with the exhaust blow-down period, followed by the exhaust stroke and later by suction stroke.

Mass flow during exhaust blow-down period

During exhaust blow-down the flow of gases out of the cylinder is due to high pressure existing within the cylinder. Mass flow rate during was calculated using the equation:

$$\frac{\mathrm{d}m}{\mathrm{d}t} = A_\mathrm{m}\sqrt{2\rho\,\mathrm{d}P} \tag{12}$$

Mass flow during displacement stroke

During displacement stroke, cylinder pressure was assumed constant and the state equation is given by $pv = m\mathrm{R}T$, for the exhaust displacement process, then:

$$\frac{\mathrm{d}V}{V} = \frac{\mathrm{d}m}{m} + \frac{\mathrm{d}T}{T} \tag{13}$$

For an adiabatic constant pressure exhaust stroke the cylinder temperature is constant.

Mass flow during suction stroke

The instantaneous mass flow rate during the suction stroke was calculated using the equation:

$$\frac{\mathrm{d}m}{\mathrm{d}t} = C_\mathrm{s} A_\mathrm{m}\sqrt{\mathrm{d}P} \tag{14}$$

where

$$C_\mathrm{S} = \sqrt{\frac{2Pi}{\mathrm{R}Ti}}$$

and suffix "*i*" refers to inlet conditions.

Test engine development

Modification of conventional turbocharged engine to LHR turbocharged engine

The conventional turbocharged engine was modified to LHR turbocharged engine through plasma spray technique. The piston crown, cylinder liner outside, cylinder head and valves are applied with partially stabilized zirconia coating of 0.5 mm thickness. Figures 1 and 2 show the photographic view of ceramic coated components.

Figure 1. Photographic view of piston top with ceramic coating

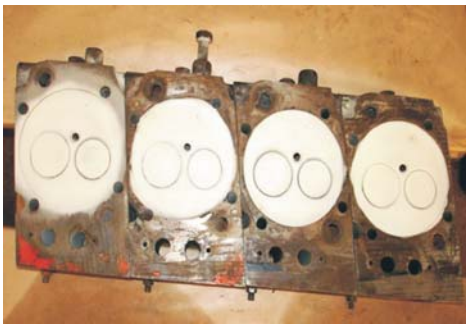

Figure 2. Photographic view of cylinder head with ceramic coating

Modification of LHR turbocharged engine to LHR turbocharged extended expansion engine

The LHR turbocharged engine was later modified to LHR turbocharged extended expansion engine by late closing of the intake valve. The intake valve closes conventionally at 45º aBDC (IVC at 45º aBDC), which was later modified to close at 60º aBDC (IVC at 60º aBDC). By late closing of the intake valve by 15º crank angle the LHR turbocharged was modified to LHR turbocharged extended expansion engine. By late closing of the intake valve the effective compression ratio was reduced from 14.18 to 12.85. Figures 3 and 4 show the valve timing diagram of the conventional turbocharged engine, LHR turbocharged extended expansion engine and figs. 5 and 6 shows the intake cam profile for the conventional turbocharged engine and modified intake cam profile for the LHR turbocharged extended expansion engine.

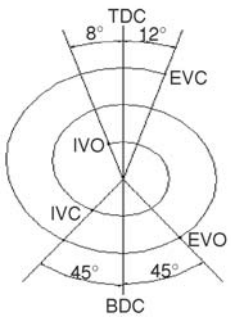

Figure 3. Conventional engine valve timing diagram

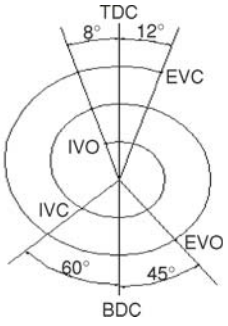

Figure 4. Extended expansion engine valve timing

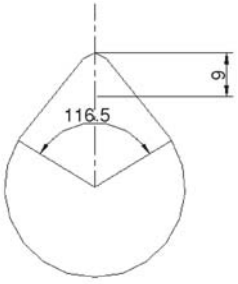

Figure 5. Conventional intake cam

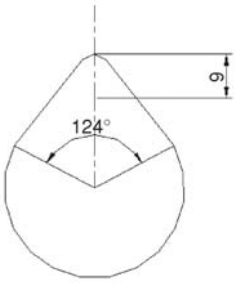

Figure 6. Modified intake cam

Modification of LHR turbocharged extended expansion engine to LHR turbocharged extended expansion engine with internal exhaust gas re-circulation

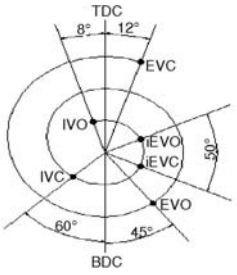

Figure 7. Turbocharged extended expansion engine with iEGR valve timing diagram

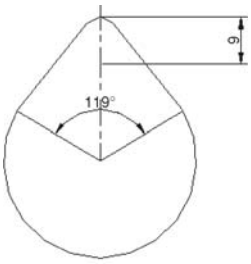

Figure 8. Conventional exhaust cam

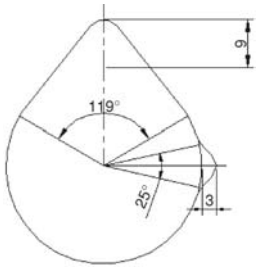

Figure 9. Modified exhaust cam with secondary lobe

The LHR turbocharged extended expansion engine was later modified to LHR turbocharged extended expansion engine with iEGR by secondary opening of the exhaust valve during suction stroke. The secondary exhaust valve opening takes place at 65º aTDC and closes at 65º bBDC. The total secondary exhaust valve opening duration is 50º crank angle (CA). The secondary exhaust valve lift is taken as 3 mm [12]. The EGR rate was determined on the basis of the engine output power with respect to the exhaust valve lift and valve opening time through the simulation. With this strategy, iEGR levels of 9 to 10% have been attained in the whole engine range. Figure 7 show the valve timing diagram for LHR turbocharged extended expansion engine with iEGR. Figures 8 and 9 show the conventional exhaust cam profile and modified exhaust cam profile.

Experimental set-up and procedure

The experimental set-up and the specifications of the test engine are shown in fig. 10 and tab. 1, respectively. The crank angle pulse generating system consisting of a pulse-generating wheel, intended to make a pulse for every 10 degrees of crank rotation is attached to the front end of the crankshaft of the engine. To distinguish the TDC and BDC position, three teeth at 5 degree gaps were provided diametrically opposite on the wheel. All other teeth were at 10 degree interval. A magnetic pick up was mounted near the pulse-generating wheel to sense the crank angle position. On rotation of the pulse generating wheel the signal generated is fed into one of the channel to the storage oscilloscope for storing and subsequently for transferring it to a personal computer for plotting the cylinder pressure with respect to crank angle. A piezo electric pressure transducer fitted with an adopter was screwed onto a tapped hole on the cylinder head. The piezo electric crystal produces an electric charge proportional to the pressure inside the combustion chamber, and this electric charge is fed to a charge amplifier for conditioning

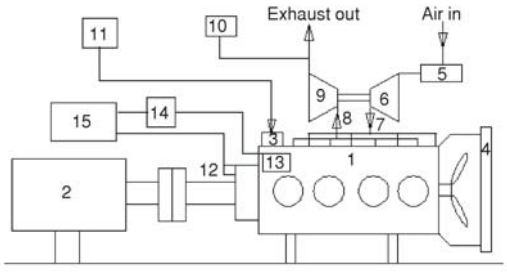

Figure 10. Experimental set-up
1 – engine, 2 – eddy current dynamometer, 3 – fuel pump, 4 – radiator, 5 – air surge tank, 6 – compressorr, 7 – inlet line, 8 – exhaust line, 9 – turbine, 10 – exhaust gas analyzer, 11 – fuel tank, 12 – crank angle encoder, 13 – piezo electric transducer, 14 – charge amplifier, 15 – digital signal explorer

and conversion into equivalent mechanical units. The output signal from the charge amplifier is fed into one channel of the storage oscilloscope for storing and transfers it to a personal computer for plotting.

The experimental engine's components such as cylinder head with valves, outer surface of the cylinder liner and the piston top surface were coated with partially stabilized zirconia of 0.5 mm thickness. After fitting the ceramic-coated components in the engine the experiments were carried out under identical conditions. The modified camshaft for extended expansion was then fitted in coated engine and the experiments were carried out under identical conditions. The modified camshaft for extended expansion with internal exhaust gas re-circulation was then fitted and the experiments were carried out under identical conditions. Under identical operating conditions the experiment was repeated for three times and precautionary steps have been taken while conducting the experiments. An uncertainty analysis was performed using the method described by Holman [29].

Table 1. Specifications of the engine

Type	4 Cylinder, 4 stroke, water cooled turbocharged DI diesel engine
Bore	111.1 mm
Stroke	127.0 mm
Connecting rod length	251.0 mm
Nominal compression ratio	16 : 1
Rated power output	55.2 kW at 1500 rpm
Fuel injection pressure	210 bar
Nozzle hole diameter	0.26 mm
No. of nozzle holes	3

Results and discussion

Tests were conducted under the following operating conditions of the engine such as (1) Conventional – Conventional turbocharged engine (IVC at 45° aBDC), (2) LHR – LHR turbocharged engine (IVC at 45° aBDC), (3) LHR (EEE) – LHR turbocharged extended expansion engine (IVC at 60° aBDC), and (4) LHR (EEE with iEGR) – LHR turbocharged extended expansion engine with iEGR (IVC at 60° aBDC with 10% EGR). The results are analysed and presented for the same fuel supplied (0.06945 g/cylinder/cycle) at 1500 rpm.

Comparison of cylinder pressure

Figure 11 shows the comparison between simulated and experimental values of cylinder peak pressure for conventional turbocharged engine, LHR turbocharged engine, LHR turbocharged extended expansion engine, and LHR turbocharged extended expansion engine with iEGR. The prediction shows that, the cylinder peak pressure are higher by 4.52% and 1.79% for LHR turbocharged engine and LHR turbocharged extended expansion engine, respectively, and is lower by 0.83% for LHR turbocharged extended expansion with iEGR when compared to conventional turbocharged engine.

The increase in cylinder peak pressure in the case of LHR turbocharged engine may be due to increased boost pressure and air density. Along with the effect of boost pressure, the higher heat retainment inside the combustion chamber with higher engine operating temperature enhances the preparation and reaction rate resulting in increased cylinder peak pressure. The cylinder peak pressure of LHR turbocharged extended expansion engine is comparatively lesser than the LHR turbocharged engine. The reason for this may be due to, reduced inlet pressure and decrease in preparation and reaction rate because of lower compression temperature caused by reduction in effective compression ratio. The cylinder peak pressure of LHR turbocharged extended expansion engine with internal exhaust gas recirculation is lower than the conventional turbo-

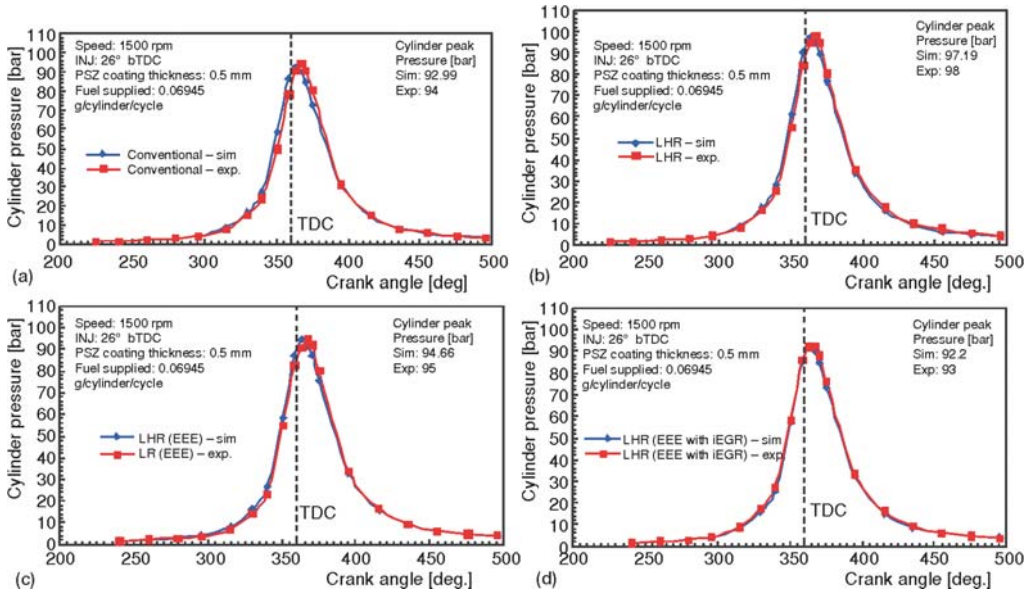

Figure 11. Comparison of cylinder pressure for different operating conditions; (a) conventional turbocharged engine, (b) LHR turbocharged engine, (c) LHR turbocharged extended expansion engine, (d) LHR turbocharged extended expansion engine with iEGR (for color image see journal web site**)**

charged engine, but it is in the operating performance limit for effective work done. The re-circulation of exhaust gas (acts as a heat sink) reduces the time availability for the mixing of the fuel with available oxygen concentration and hence the mixing and preparation is reduced. This variation in charge mixing and preparation rate and reduction in compression ratio results in reduction in pressure in LHR turbocharged extended expansion engine with iEGR.

Comparison of cylinder mean temperature

Cylinder mean temperature is the cylinder area averaged temperature which is lower than the peak flame temperature and which is essentially responsible for the work done. Figure 12 shows the comparison of cylinder mean temperature for conventional turbocharged engine, LHR turbocharged engine, LHR turbocharged extended expansion engine, and LHR turbocharged extended expansion engine with iEGR. The percentage increase in cylinder mean temperature for LHR turbocharged engine, LHR turbocharged extended expansion engine, and LHR turbocharged extended expansion with iEGR are 6.03%, 4.48% and 3.75%, respectively, when compared to conventional turbocharged engine. The trend shows that LHR turbocharged engines are operating at higher cylinder mean temperature. The higher cylinder mean temperature achieved is mainly attributed to insulation coatings applied to combustion chamber walls.

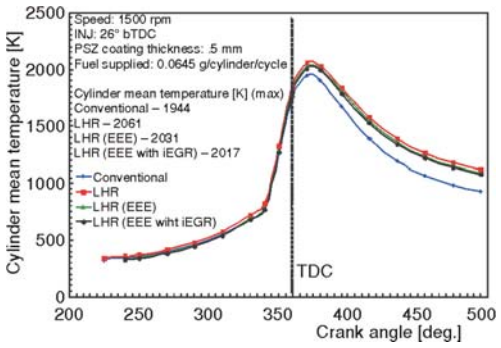

Figure 12. Comparison of cylinder mean temperature for different operating conditions (for color image see journal web site**)**

In the case of LHR turbocharged extended expansion engine due to reduction in effective compression ratio, the compression temperature decreases leading to lesser rate of heat release, thereby decreasing the heat content inside the cylinder which finally results in lower cylinder mean temperature. In the case of LHR turbocharged extended expansion engine with iEGR, because of the re-circulation of the exhaust gases mainly CO_2 and H_2O (gaseous) the specific heat of the cylinder gases increases, which decreases the cylinder mean temperature when compared to the LHR turbocharged extended expansion engine. The amount of exhaust gas re-circulated was small in portion. If higher percentages of exhaust gas is re-circulated the engine performance gets affected, so with a restriction of 10% of EGR was assumed in this work to avoid the NO_x formation which results in only a small effect with the variation in the cylinder mean temperature.

Comparison of rate of heat release

Figure 13 shows the comparison of rate of heat release for Conventional turbocharged engine, LHR turbocharged engine, LHR turbocharged extended expansion engine and LHR turbocharged extended expansion engine with iEGR. The prediction shows that the peak rate of heat releases during premixed combustion are lower by 31.43% and 8.93% for LHR turbocharged engine and LHR turbocharged extended expansion engine respectively and is higher by 0.84% for LHR turbocharged extended expansion with iEGR when compared to conventional turbocharged engine. The experimental values of peak rate of heat release when compared to theoretical predictions are lesser by 6.14%, 6.71%, 5.32%, and 6.42% for Conventional turbocharged engine, LHR turbocharged engine, LHR turbocharged extended expansion engine and LHR turbocharged extended expansion engine with iEGR, respectively.

The decrease in peak rate of heat release during premixed combustion in the case of LHR turbocharged engine compared to Conventional turbocharged engine is due to decrease in

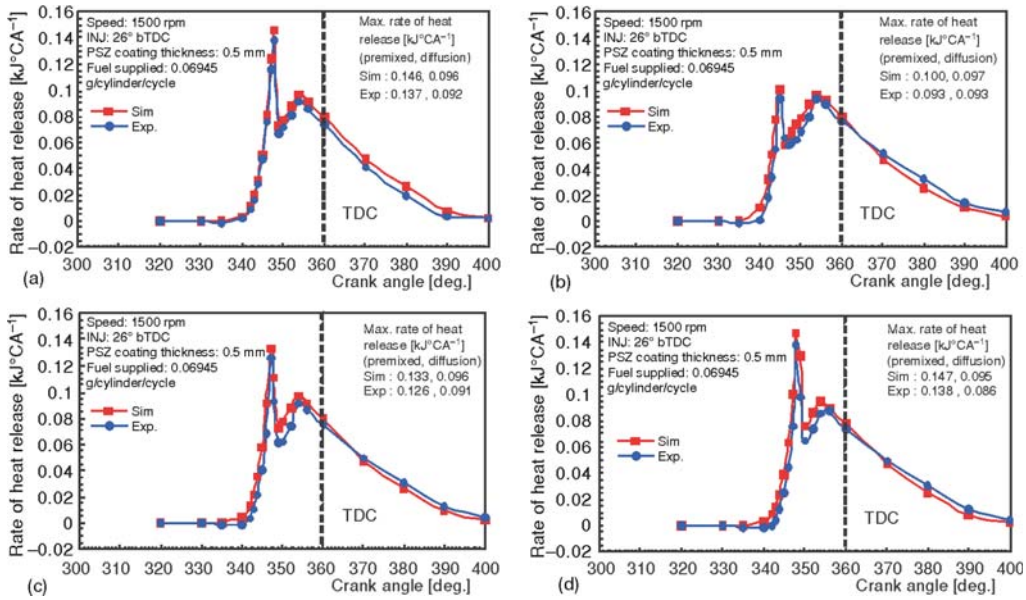

Figure 13. Comparison of rate of heat release for different operating conditions; (a) conventional turbocharged engine, (b) LHR turbocharged engine, (c) LHR turbocharged extended expansion engine, (d) LHR turbocharged extended expansion engine (for color image see journal web site**)**

time available for charge mixing and preparation because of higher heat retainment inside the combustion chamber leading to instantaneous burning of fuel at much elevated temperatures. The increase in peak heat release during premixed combustion in the case of LHR extended expansion engine is due to lower preparation rate along with proportionate amount of charge accumulation and its spontaneous burning. As in the case of LHR extended expansion engine with iEGR the above charge accumulation may be further more increased and burnt spontaneously which leads to further increase in peak rate of heat release.

Comparison of cumulative work done

Figure 14 shows the comparison of cumulative work done for conventional turbocharged engine, LHR turbocharged engine, LHR turbocharged extended expansion engine, and LHR turbocharged extended expansion engine with iEGR. The prediction shows that the cumulative work done for LHR turbocharged engine and LHR turbocharged extended expansion engine and LHR turbocharged extended expansion with iEGR is higher by 5.42%, 5.82%, and 3.35%, respectively, when compared to conventional turbocharged engine. The increase in the cumulative work done in the case of LHR turbocharged extended expansion engine is mainly attributed to the decrease in compression work done. The compression work done reduces by 8.01% for LHR turbocharged extended expansion engine when compared to LHR turbocharged engine. The cumulative work done of LHR turbocharged extended expansion engine with iEGR is lesser than the LHR turbocharged extended expansion engine. This may be due to lower cylinder peak pressure but it is in the operating performance limit for effective work done.

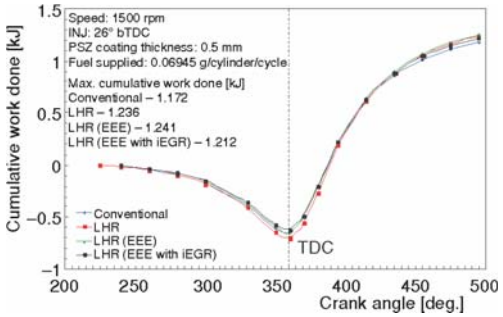

Figure 14. Comparison of work done for different operating conditions
(for color image see journal web site**)**

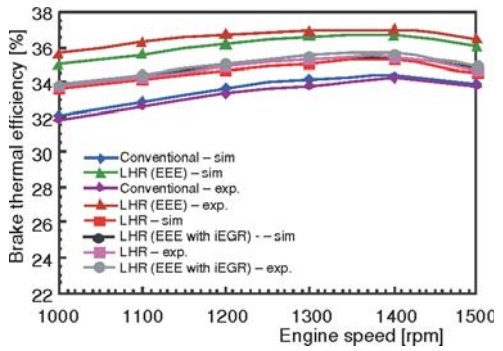

Figure 15. Variation of brake thermal efficiency with respect to engine speed
(for color image see journal web site**)**

Brake thermal efficiency

Figure 15 shows the variation of brake thermal efficiency with speed. The brake thermal efficiency increases by 1.71% to 4.58% for LHR turbocharged engine, 6.26% to 9.07% for LHR turbocharged extended expansion engine and 2.73% to 4.90% for LHR turbocharged extended expansion engine with iEGR when compared to conventional turbocharged engine for the speed range of 1000 rpm to 1500 rpm. Experimental results are also in close agreement with the simulation results and the corresponding values are 2.80% to 5.74%, 8.03% to 11.88%, and 3.55% to 6.33%, respectively. In the case of LHR turbocharged extended expansion engine the brake thermal efficiency increases compared to conventional turbocharged engine due to decrease in heat transfer and compression work done caused by ceramic coating and late closing of the intake valve respectively. In the case of LHR extended expansion engine

with iEGR the brake thermal efficiency decreases when compared to LHR turbocharged extended expansion engine because of the replacement of fresh charge with EGR, which decreases the cylinder peak pressure, resulting in decrease in cumulative work done. But the brake thermal efficiency of LHR turbocharged extended expansion engine with iEGR is higher than the conventional turbocharged engine.

NO_x emissions

Figure 16 shows the comparison of NO_x emissions with speed. The trend shows that the NO_x emission increases with increasing speed for all operating conditions. The NO_x emissions increases by about 50.18% and 25.33% for LHR turbocharged engine and LHR turbocharged extended expansion, respectively, and reduces by 7.03% for LHR turbocharged extended expansion engine with iEGR when compared to conventional turbocharged engine at 1500 rpm. In low heat rejection engines due to higher peak flame temperature dissociation of N_2 and O_2 takes place within a short period of time, which increases the formation of NO_x emission. The decrease in NO_x emissions in LHR turbocharged extended expansion engine with iEGR is more significant due to its lower operating temperature and lesser oxygen concentration. The results of the computations show the expected behaviour and are qualitatively and quantitatively in excellent agreement with the experiment.

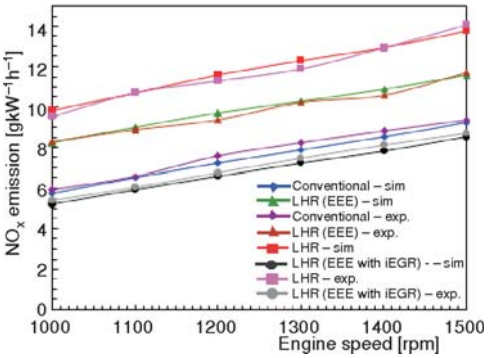

Figure 16. Variation of NO_x emissions with respect to engine speed
(for color image see journal web site**)**

Hydrocarbon emissions

Figure 17 shows the comparison of hydrocarbon emissions with speed. The hydrocarbon emissions reduces by 32.45% and 17.9% for LHR turbocharged engine and LHR turbocharged extended expansion engine, respectively, and increases by 2.06% for LHR turbocharged extended expansion engine with iEGR when compared to conventional turbocharged engine at 1500 rpm. Experimental results are also in close agreement with the simulation results and the corresponding values are 21.54%, 14.89% and 3.24%, respectively.

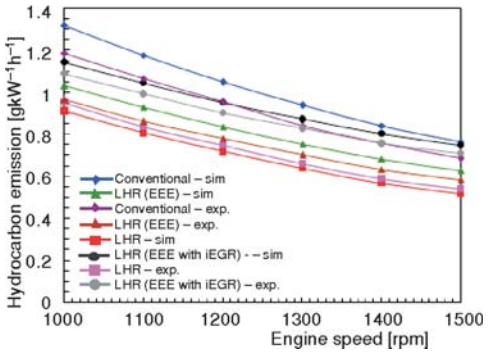

Figure 17. Variation of hydrocarbon emissions with respect to engine speed
(for color image see journal web site**)**

Conclusions

After a detailed analysis of the conventional turbocharged engine, LHR turbocharged engine, LHR turbocharged extended expansion engine, and LHR turbocharged extended expansion engine with iEGR, focusing on combustion, performance, and emissions the following conclusions were made.

- The in-cylinder peak pressure for LHR turbocharged extended expansion engine with iEGR is lower by 0.83% when compared to conventional turbocharged engine, but it is in the operating performance limit for effective work done.

- The cylinder mean temperature for LHR turbocharged extended expansion engine with iEGR is higher by 3.75% when compared to conventional turbocharged engine. The high temperature achieved is mainly attributed to insulation coating applied to cylinder components.
- The rate of heat release during premixed combustion is higher by 0.84% for LHR turbocharged extended expansion with iEGR when compared to conventional turbocharged engine may be due to increase in ignition delay period because of the lesser preparation rate caused by reduced oxygen concentration.
- The cumulative work done is higher by 3.35% for LHR turbocharged extended expansion engine with iEGR when compared to conventional turbocharged engine because of lower compression work done.
- NO_x emission increases with increasing speed for all operating conditions. It decreases by 7.03% for LHR turbocharged extended expansion engine with iEGR when compared to conventional turbocharged engine at 1500 rpm.
- The hydrocarbon emissions slightly increases by 2.06% for LHR turbocharged extended expansion engine with iEGR when compared to conventional turbocharged engine.

The comparison of predicted and measured data demonstrated reasonable quantitative agreement between them. Additional effort is required to assess the fidelity of each model across a wider range of operating conditions and engine types.

Nomenclature

A_m – minimum valve flow area, [m^2]
A_n – nozzle hole area, [m^2]
a, b, c, d – Annand's convective heat transfer equation co-efficient
C_d – coefficient of discharge for injector nozzle
C_s – parameter for mass flow through the intake valve
d_n – nozzle hole diameter, [mm]
h – number of holes in injector nozzle
h_c – wall – coolant heat transfer coefficient, [kJm^{-2}h^{-1}K^{-1}]
h_g – gas wall heat transfer coefficient, [kJm^{-2}h^{-1}K^{-1}]
K – constant in preparation rate equation
k – thermal conductivity, [Wm^{-1}K^{-1}]
k_c – thermal conductivity of ceramic material, [WmK^{-1}]
k_l – thermal conductivity of liner material, [WmK^{-1}]
k_p – thermal conductivity of piston material, [WmK^{-1}]
k_r – thermal conductivity of ring material, [WmK^{-1}]
L – index constant in preparation rate equation
l – stroke length, [m]
l_l – cylinder length, [m]
l_C – connecting rod length, [m]
l_s – skirt length, [m]
M – mass of fuel injected, [grams/cycle/cylinder]
M_i – total mass of fuel injected, [kg]
M_u – mass of fuel in cylinder and unprepared, [kg]
m_f – mass of fuel injected during injection period for each cylinder, [kg]
P_i – injection period, [degree crank angle]
P_r – preparation rate, [kg per degree crank angle]
Δp – pressure drop across the nozzle, [bar]
Q – total heat transfer, [kJ]
Q_w – wall heat transfer, [kJ]
R_r – reaction rate, [kg per degree crank angle]
$r_1, r_2, r_3, r_4, r_5, r_6, r_7, r_8, r_9$ – radii of the composite cylinder wall with respect to cylinder axis, [m]
T_c – cylinder mean temperature, [K]
T_g – gas temperature, [K]
T_p – thickness of the piston crown, [m]
T_w – cylinder wall temperature, [K]
x – index constant in preparation rate equation

References

[1] Baluswamy, N., Spatial and Temporal Distribution of Gaseous Pollutants in a Diesel Engine Combustion Chamber, Ph. D. thesis, Institute of Sc. Tech., University of Manchester, Manchester, UK, 1976

[2] Buyukkaya, E., *et al*., Effects of Thermal Barrier Coating on Gas Emissions and Performance of a LHR Engine with Different Injection Timings and Valve Adjustments, *Energy Conversion and Management, 47* (2006), 9-10, pp. 1298-1310
[3] Parlak, A., *et al*., The effects of Injection Timing on NO_x Emissions of a Low Heat Rejection Indirect Diesel Injection Engine, *Applied Thermal Engineering, 25* (2005), 17-18, pp. 3042-3052
[4] Kesava Reddy, Ch., *et al*., Performance Evaluation of a Low-Grade Low-Heat-Rejection Diesel Engine with Crude Pongamia Oil, *ISRN Renewable Energy, 2012* (2012), ID 489605
[5] Rajendra Prasath, B., *et al*., Two-Zone Modeling of Diesel/Biodiesel Blended Fuel Operated Ceramic Coated Direct Injection Diesel Engine, *International Journal of Energy and Environment, 1* (2010), 6, pp. 1039-1056
[6] Mathews, P. K., Deepanraj, B., Experimental Investigation on Performance and Emission Characteristics of Low Heat Rejection Diesel Engine with Ethanol as Fuel, *American Journal of Applied Sciences, 8* (2011), 4, pp. 348-354
[7] Shrirao, P. N., Pawar, A. N., Evaluation of Performance and Emission Characteristics of Turbocharged Diesel Engine with Mullite as Thermal Barrier Coating, *International Journal of Engineering and Technology, 3* (2011), 3, pp. 256-262
[8] Tamil Porai, P., *et al*., Simulation and Analysis of Combustion and Heat Transfer in Low-Heat-Rejection Diesel Engine Using Two-Zone Combustion Model and Different Heat Transfer Models, SAE technical paper 2003-01-1067, 2003
[9] Parlak, A., *et al*., The Effect of Thermal Barrier Coating on a Turbo-Charged Diesel Engine Performance and Exergy Potential of the Exhaust Gas, *Energy Conversion and Management, 46* (2005), 3, pp. 489-499
[10] Giakoumis, E. G., Cylinder Wall Insulation Effects on the First and Second-Law Balances of a Turbocharged Diesel Engine Operating under Transient Load Conditions, *Energy Conversion and Management 48* (2007), 11, pp. 2925-2933
[11] Kentfield, J. A. C., Diesel Engines with Extended Expansion Strokes, SAE paper 891866, 1989
[12] Kamo, R., *et al*., Emissions Comparisons of an Insulated Turbocharged Multi-Cylinder Miller Cycle Diesel Engine, SAE paper 980888, 1998
[13] Mavinahally, N., Kamo, R., Insulated Miller Cycle Diesel Engine, SAE paper 961050, 1996
[14] Jafarmadar, S., Hosseinzadeh, M., Iimprovement of Emissions and Performance by using of Air Jet, Exhaust Gas Re-Circulation and Insulation Methods in a Direct Injection Diesel Engine, *Thermal Science,17* (2013), 1, pp. 57-70
[15] Khatamnezhad, H., *et al*., Incorporation of Exhaust Gas Recirculation and Split Injection for Reduction of NO_x and Soot Emissions in Direct Injection Diesel Engines, *Thermal Science, 15* (2011), Suppl. 2, pp. S409-S427
[16] Benajes, J., *et al.*, Potential of Atkinson Cycle Combined with EGR for Pollutant Control in a HD Diesel engine Energy Conversion and Management, *50* (2009), 1, pp. 174-183
[17] Yousufuddin, S., *et al*., A Computational Study to Investigate the Effects of Insulation and EGR in a Diesel engine, *International Journal of Energy and Environment, 3* (2012), 2, pp. 247-266
[18] Abd-Alla, G.H, Using Exhaust Gas Recirculation in Internal Combustion Engines: A Review, *Energy Conversion and Management, 43* (2002), 8, pp. 1027-1042
[19] Edwards, S. P., *et al*., The Potential of a Combined Miller Cycle and Internal EGR Engine for Future Heavy Duty Truck Applications, SAE paper 980180, 1998
[20] Yilmaz, H., Stefanopoulou, A., Control of Charge Dilution in Turbocharged Diesel Engines via Exhaust Valve Timing, *Journal of Dynamic Systems, Measurement, and Control, 127* (2005), September, pp. 363-373
[21] Brunt, M., Platts, K., Calculation of Heat Release in Direct Injection Diesel Engines, SAE technical paper 1999-01-0187, 1999
[22] Brunt, M., Platts, K., Calculation of Heat Release in Direct Injection Diesel Engines, SAE technical paper 1999-01-0187
[23] Annand, W. J. D., Heat Transfer in the Cylinders of Reciprocating Internal Combustion Engines, *Proc. I. Mech. E. London, Vol. 177* (1963), 36, pp. 973-996
[24] Rajendra Prasath, B., *et al*., Analysis of Combustion, Performance and Emission Characteristics of Low Heat Rejection Engine Using Biodiesel, *International Journal of Thermal Science, 49* (2010), 3, pp. 2483-2490
[25] Amann, C. A., Promises and Challenges of the Low Heat Rejection Diesel, *ASME, Journal of Engineering for Gas Turbine and Power, 110* (1988), pp. 475-481.

[26] Miyairi, Y., Computer Simulation of an LHR DI Diesel Engine, SAE paper 880187, 1988
[27] Heywood, J. B., *Internal Combustion Engine Fundamentals*, McGraw-Hill Book Co., New York, USA, 1988
[28] Benson, R. S., Whitehouse, N. D., *Internal Combustion Engines*, Pergamon Press, Oxford, UK, 1979
[29] Holman, J. P., *Experimental Methods for Engineers*, McGraw-Hill Book Co., New York, USA, 2001

Paper submitted: July 7, 2013
Paper revised: January 6, 2014
Paper accepted: Januay 7, 2014